Crossover from non-Fermi liquid to Fermi liquid behavior and the superconductivity dome in heavy electron systems

P. Schlottmann

Florida State University

Dept. of Physics and NHMFL

Tallahassee, Florida

Supported by the US Department of Energy

Grant No. DE-FG02-98ER45707

I. Motivation

Normal metals: Landau's Fermi liquid theory

- Resistivity: $\rho(T) = \rho_0 + AT^2$
- Specific heat: $C = ⅓\, m^* p_0 T$
- Enhanced Pauli susceptibility

Non-Fermi-liquid behavior: (anomalous metals)

deviations from Fermi liquid; power laws or log-dependence in specific heat, magnetization, resistivity, etc.

Quantum critical point; no universality

Examples :

$CePd_2Si_2$, $CeIn_3$

$CeCu_{5.9}Au_{0.1}$, $YbRh_2Si_2$, $CeAuSb_2$

more than 100 known compounds and alloys

$CeCu_{6-x}Au_x$

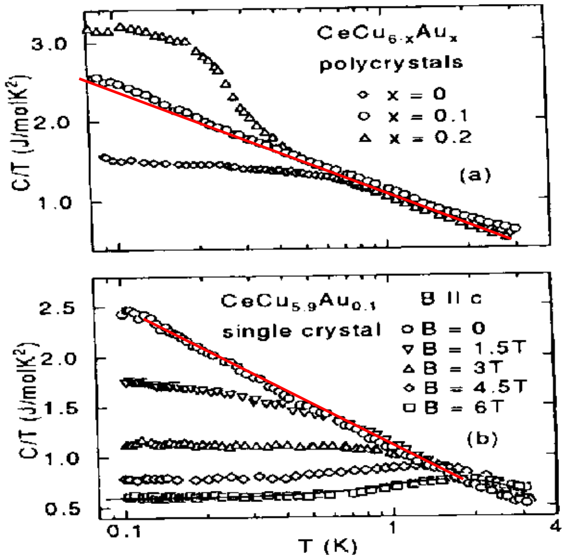

FIG. 1. (a) Specific heat C plotted as C/T vs temperature T (semilog) of $CeCu_{6-x}Au_x$ polycrystals. (b) C/T vs T (semilog) for a $CeCu_{5.9}Au_{0.1}$ single crystal for different magnetic field B applied to the easy direction. Solid line for $B=6$ T indicates fit of the resonance-level model (see text).

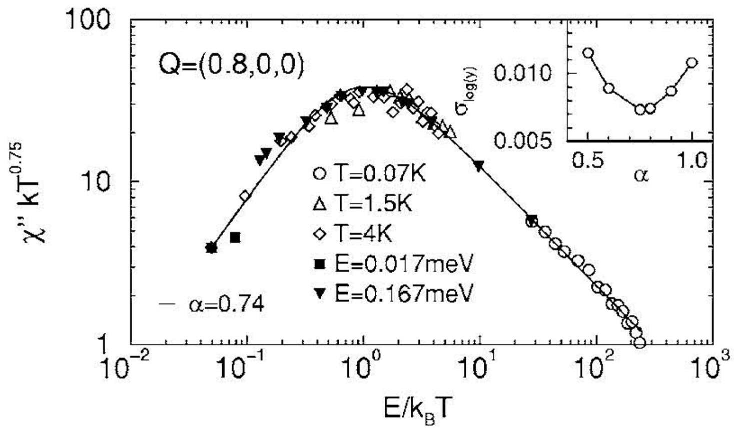

FIG. 12. Scaling plot of inelastic neutron-scattering data for $CeCu_{5.8}Au_{0.2}$ at $\mathbf{q}=(0.8\ 0\ 0)$ vs E/k_BT. Solid line corresponds to a fit of the scaling function Eq. (150) with $\alpha=0.74$. Inset: The quality of the scaling collapse varying with α. From Schröder *et al.*, 1998.

Dynamical susceptibility: E/T scaling

$$X^{-1}(\mathbf{q},E,T) = c^{-1}\{f(\mathbf{q}) + (-iE+aT)^{\alpha}\} \ ; \ \alpha = 0.74$$

"local critical behavior"

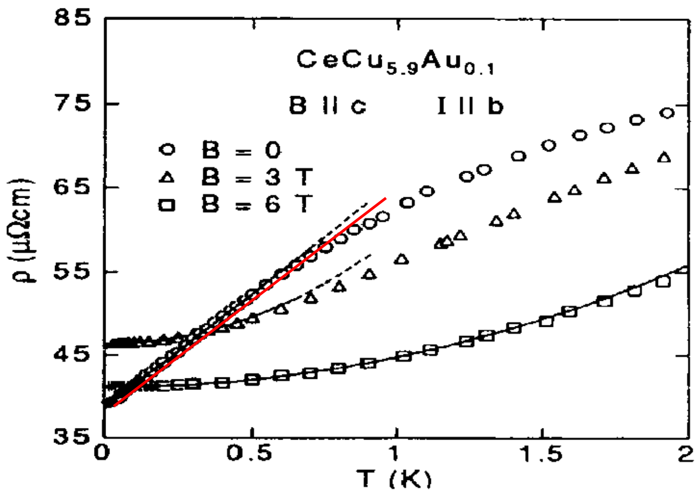

FIG. 3. Electrical resistivity ρ vs temperature T of $CeCu_{5.9}Au_{0.1}$ for different magnetic fields B applied to the easy direction. Solid lines indicate fits with a T-linear ($B=0$) and T^2 dependence ($B=3$ and 6 T).

H. von Löhneysen et al, PRL **72**, 3262 (1994)

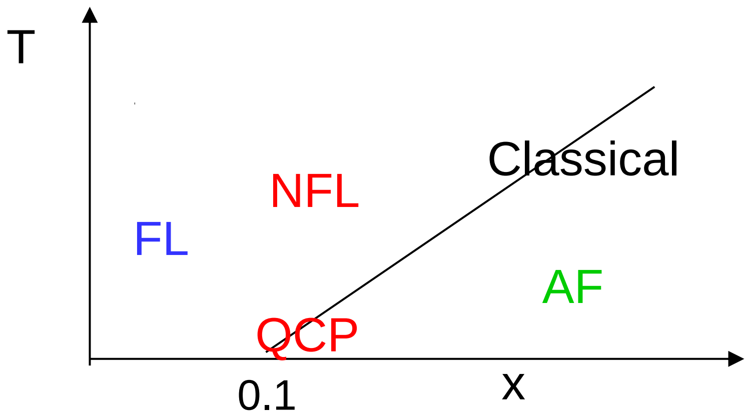

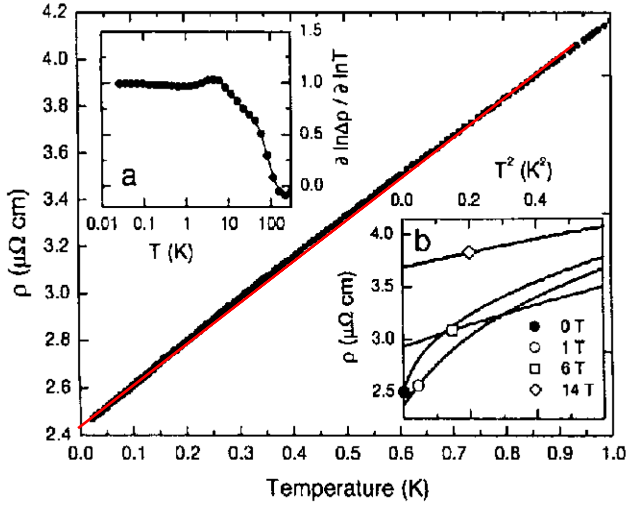

FIG. 2. Low-temperature electrical resistivity of $YbRh_2Si_2$ at $p = 0$ measured along the a axis as a function of temperature, obeying $\rho(T) = \rho_0 + bT^{\varepsilon}$, with $\varepsilon \simeq 1$. (a) Temperature dependence of the effective exponent ε, defined as the logarithmic derivative of $\Delta\rho = \rho - \rho_0$ with respect to T. (b) $\rho(T)$, plotted as ρ vs T^2, for $B \leq 14$ T applied along the c axis. The position of the symbols indicates the crossover temperature below which a T^2 law is recovered.

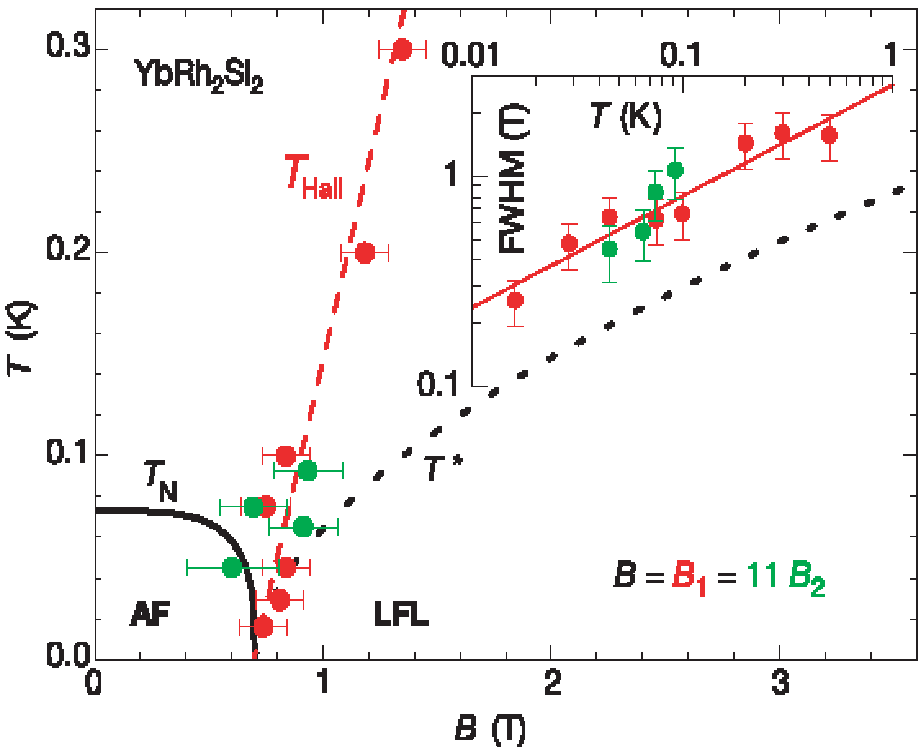

Hall effect and small vs large FS

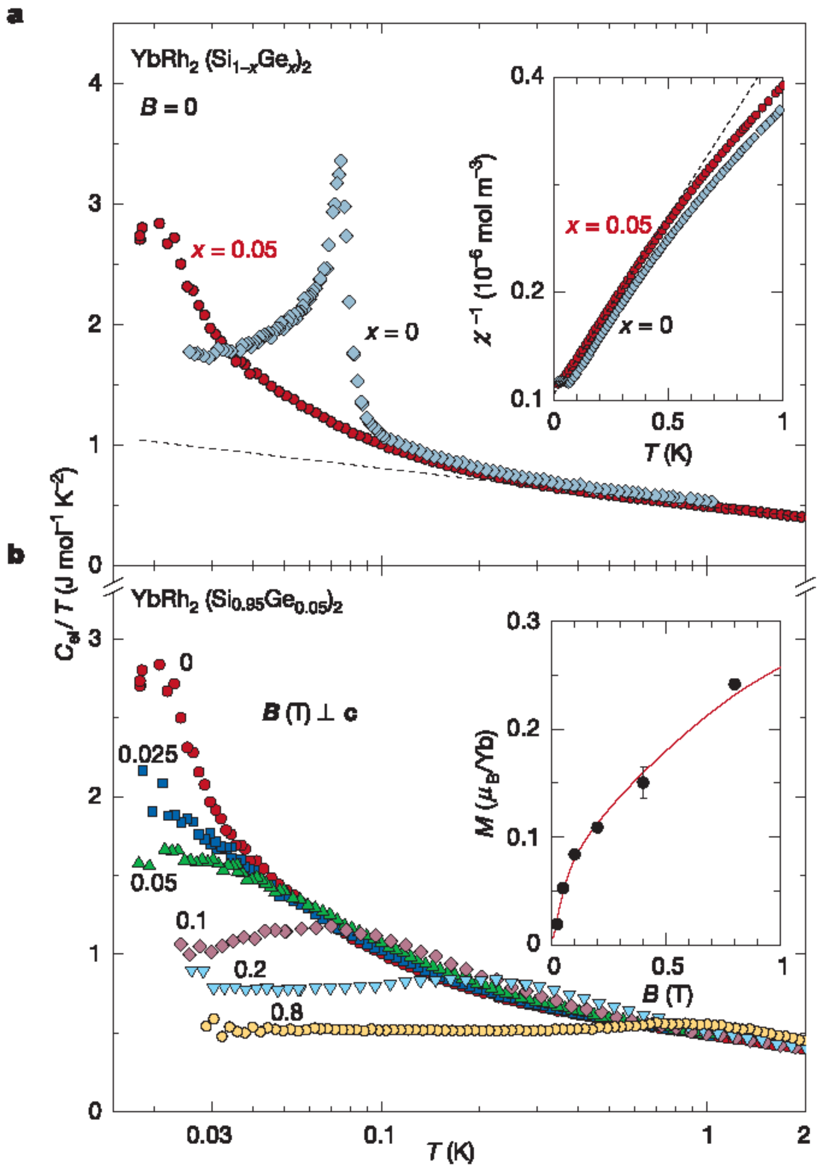

$YbRh_2Si_2$ Field-tuned transition

Trovarelli et al, PRL (2000)
Gegenwart et al, PRL (2002)
Custers et al, Nature (2003)
Paschen et al, Nature (2004)

Non-Fermi liquid behavior and a superconducting dome

Systems with QCP somewhat related to the Hertz-Millis-Moriya theory

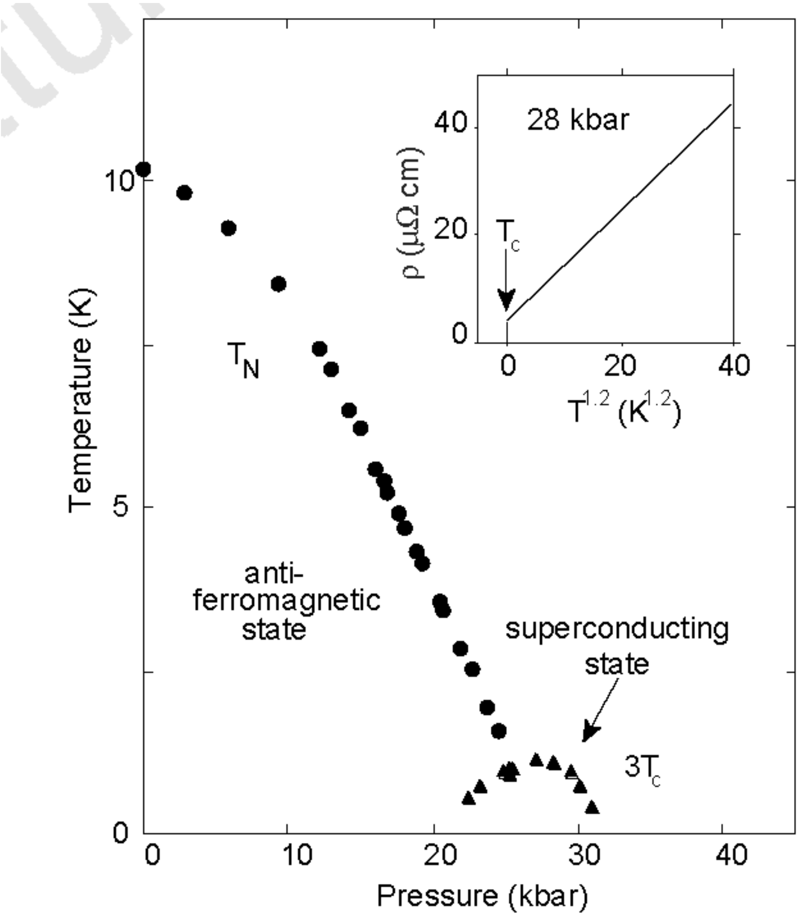

$CePd_2Si_2$

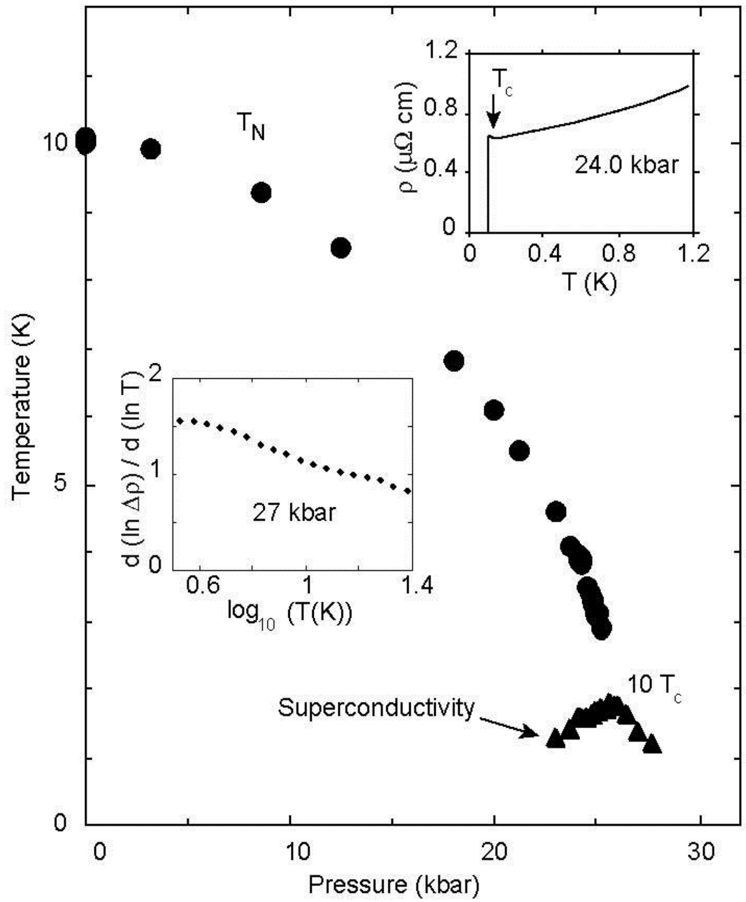

$CeIn_3$

Mathur, Grosche, Julian, Walker, Freye, Haselwimmer and Lonzarich, Nature (1998)

II. Model

- Strong correlations in rare earth (actinide) systems
  → bands of heavy quasi-particles (heavy fermions)
- weak remaining repulsive interaction after heavy quasi-particles are formed (Landau's FL theory)
- nesting of FS and remaining interactions yield itinerant AF
- $T_N \to 0$ yields QCP

Two heavy-electron pockets separated by **Q**

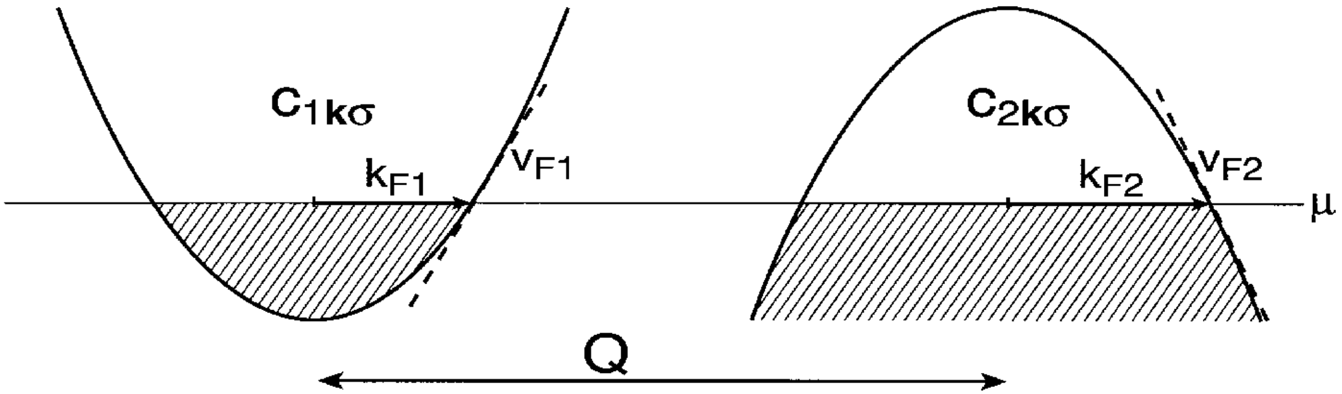

electrons

$\varepsilon_1(k)=k^2/2m$

holes

$\varepsilon_2(k)=E_0-k^2/2m$

Interaction:

$$
\begin{aligned}
H_{int} &= \sum_{j\mathbf{k}\mathbf{k}'\mathbf{q}\sigma\sigma'} W_j(\mathbf{q}) c^\dagger_{j\mathbf{k}\sigma} c_{j\mathbf{k}+\mathbf{q}\sigma} c^\dagger_{j\mathbf{k}'+\mathbf{q}\sigma'} c_{j\mathbf{k}'\sigma'} \\
&+ \sum_{\mathbf{k}\mathbf{k}'\mathbf{q}\sigma\sigma'} V(\mathbf{q}) c^\dagger_{1\mathbf{k}+\mathbf{q}\sigma} c_{1\mathbf{k}\sigma} c^\dagger_{2\mathbf{k}'-\mathbf{q}\sigma'} c_{2\mathbf{k}'\sigma'} \\
&+ \sum_{\mathbf{k}\mathbf{k}'\mathbf{q}\sigma\sigma'} U(\mathbf{Q}) c^\dagger_{1\mathbf{k}+\mathbf{q}\sigma} c^\dagger_{2\mathbf{k}'-\mathbf{q}\sigma'} c_{1\mathbf{k}\sigma'} c_{2\mathbf{k}'\sigma} \\
&+ \sum_{\mathbf{k}\mathbf{k}'\mathbf{q}\sigma\sigma'} P(2\mathbf{Q}) [c^\dagger_{1\mathbf{k}+\mathbf{q}\sigma} c^\dagger_{1\mathbf{k}'-\mathbf{q}\sigma'} c_{2\mathbf{k}'\sigma'} c_{2\mathbf{k}\sigma} + H.c.]
\end{aligned}
$$

Hubbard limit:

W=V=U=P

P is Umklapp only active if Q = G/2; pairs of electrons: superconductivity

Consider first case where Q is not commensurate with lattice

Mean-field

- nesting of FS → SDW or CDW
- BCS-like equation with gap Δ , T_c maximum for perfect nesting
- nesting mismatch increasing $|k_{F2} - k_{F1}|$ reduces T_c and Δ → QCP
- logarithms to all order of perturbation

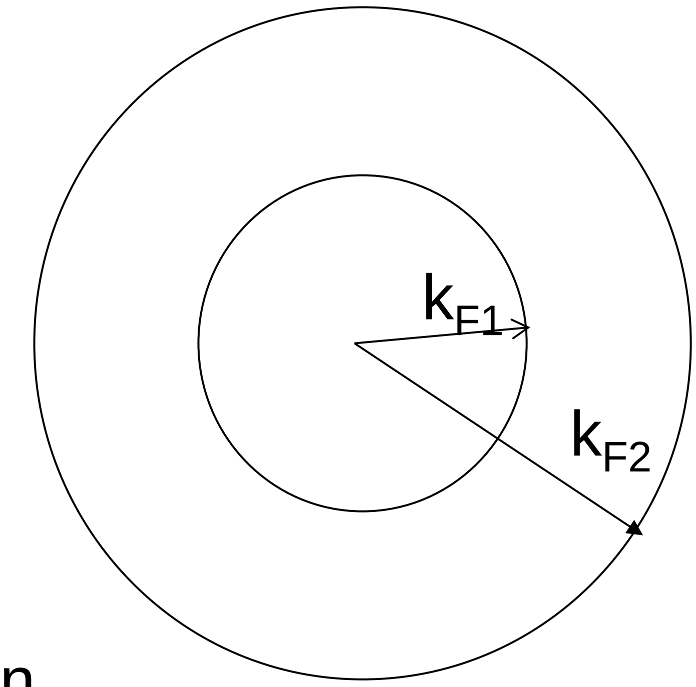

III. Renormalization Group

(a) Multiplicative RG (b) Wilsonian RG

- eliminates electronic degrees of freedom

$$-\Lambda \leq k \leq \Lambda \quad \rightarrow \quad -(\Lambda - d\Lambda) \leq k \leq (\Lambda - d\Lambda)$$

- energy variable : $t = \ln(\Lambda_0 / \Lambda)$
- sums the log-terms consistently

RG-flow diagram

- weak-coupling

  fixed point U=V=0
- strong-coupling fixed points

Instabilities:

V > 0 SDW

V - 2 U > 0 CDW

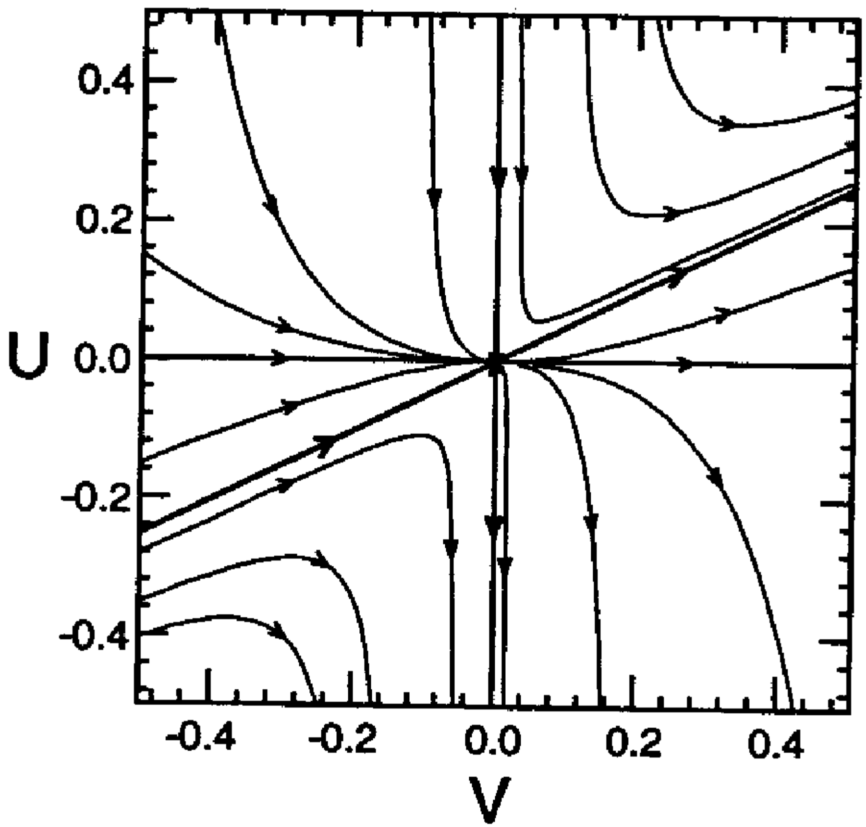

IV. Results

$\delta = ½\,|k_{F2} - k_{F1}|\,v_F$

is Fermi surface mismatch

$U\rho_F = 0.2, \quad v_F\,\Lambda_0 = 10$

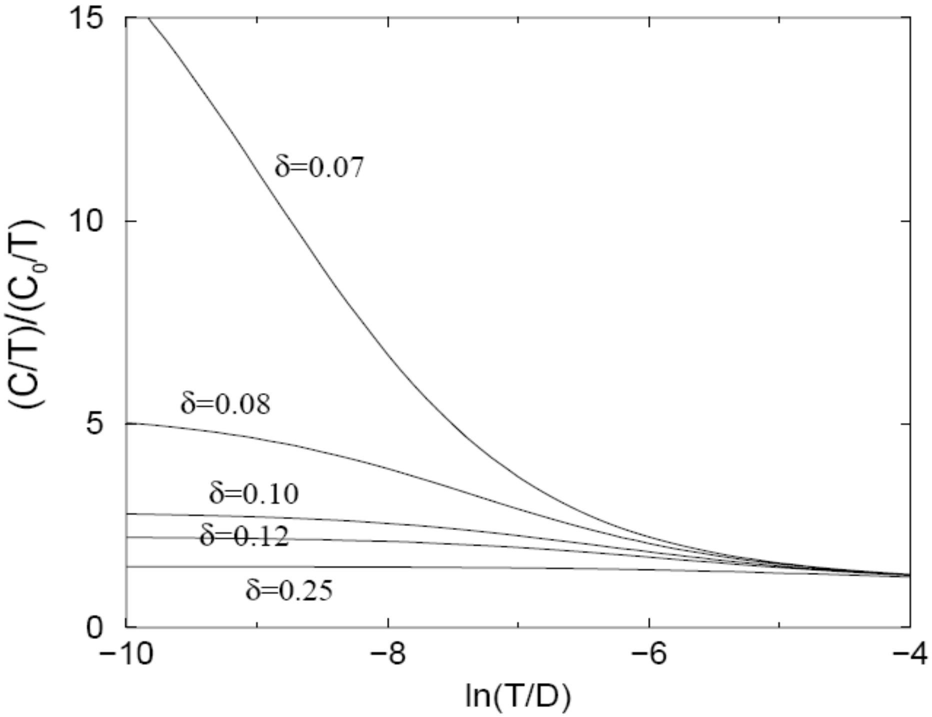

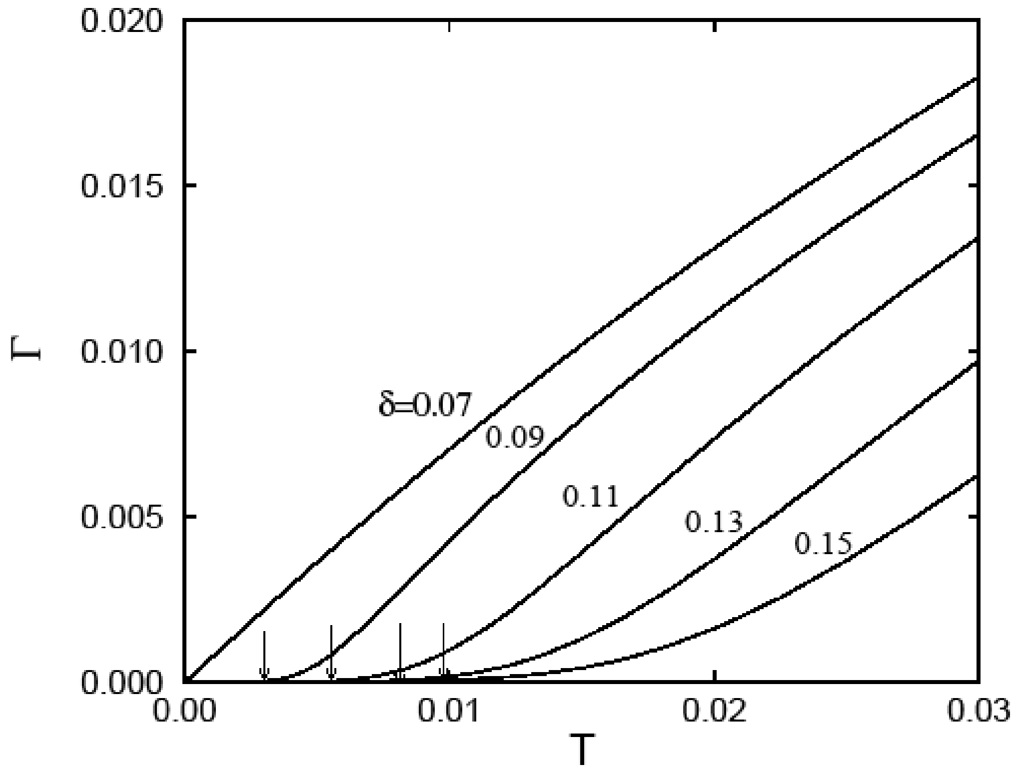

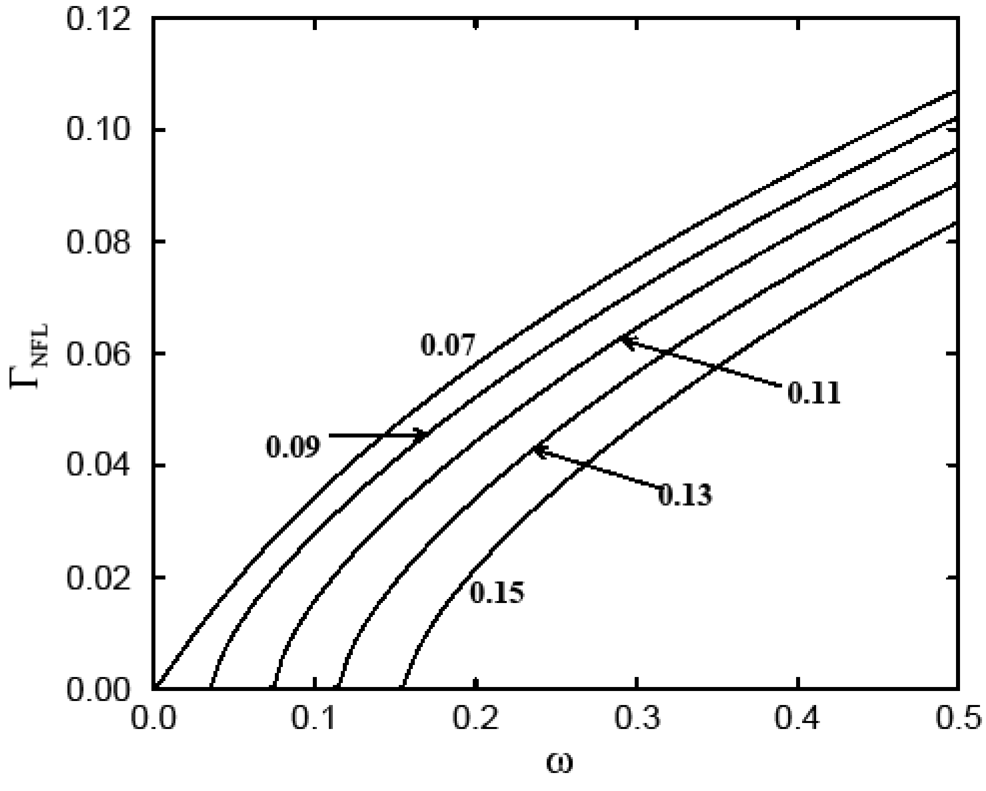

Specific heat and quasi-particle line-width: Crossover from FL to NFL

Crossover from FL to NFL

Phase diagram:

(from specific heat and line-width)

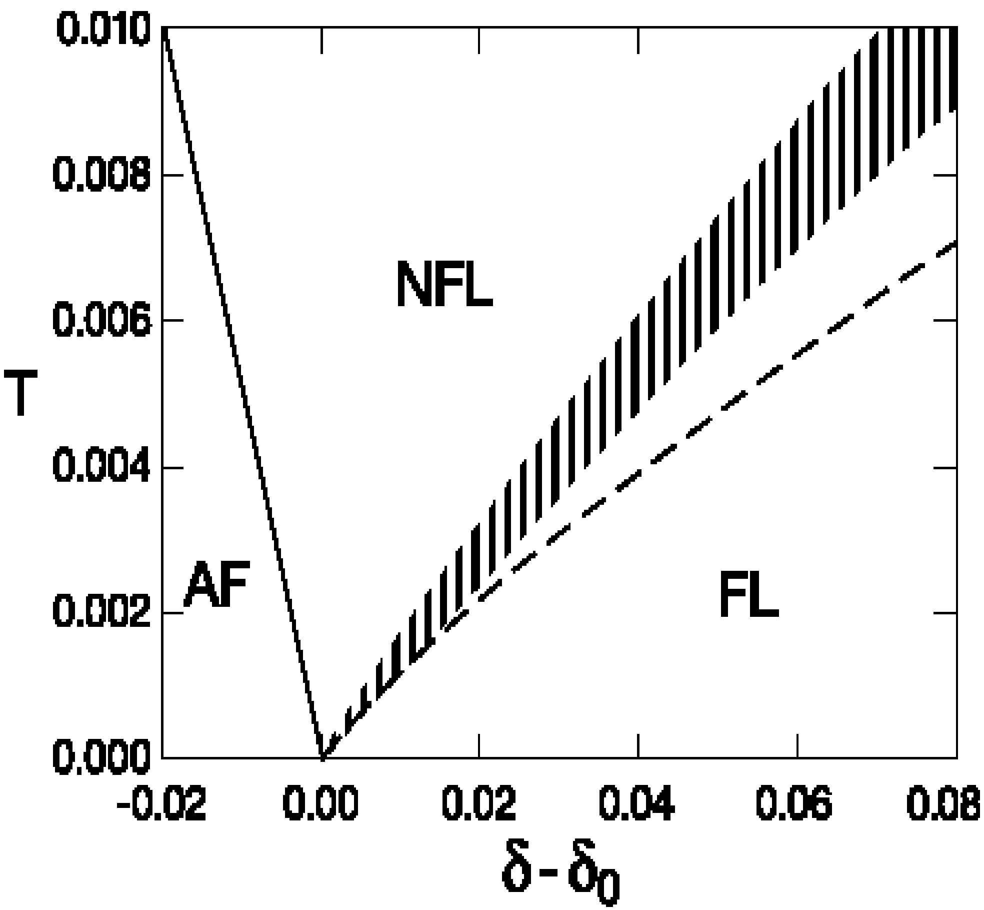

Phase diagram:

$YbRh_2Si_2$

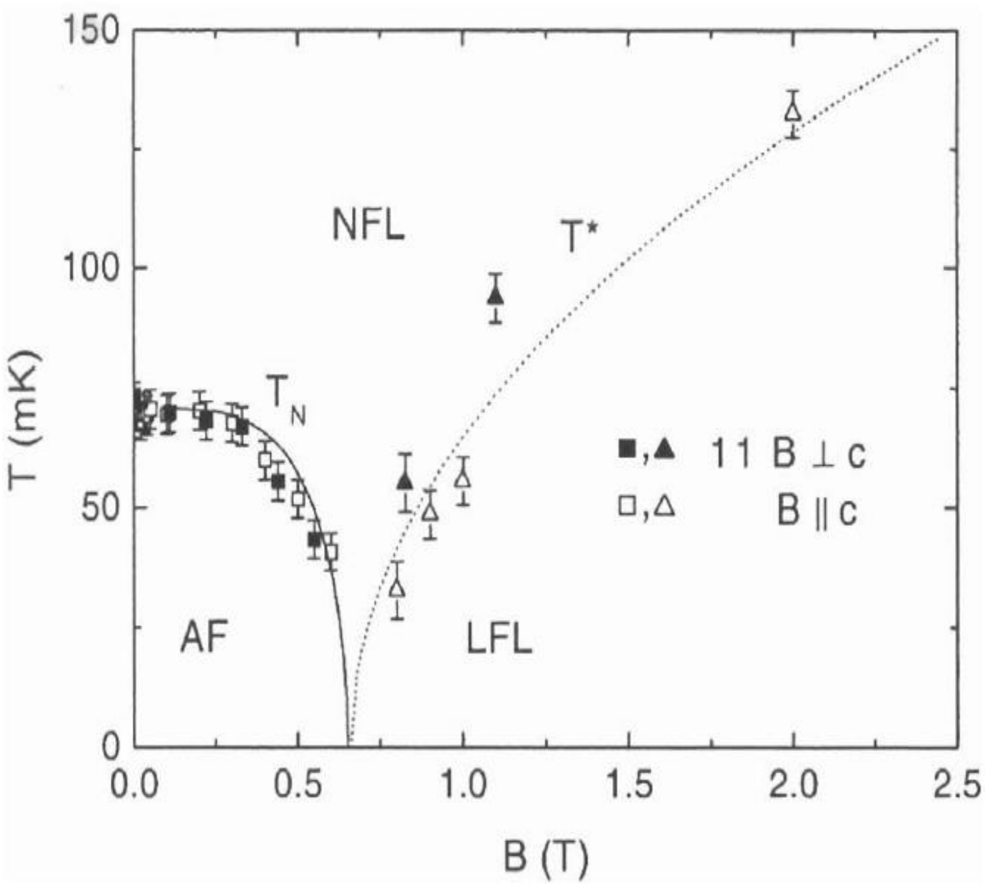

V. Superconductivity: Q=G/2

- Pairs of electrons can be transferred between pockets
- Similar to iron pnictides (Chubukov (2009))
- Six interaction vertices (rather than three) lead to six order parameters; four of them are relevant

$$\mathcal{O}_{SDW} = \sum_{\mathbf{k}} \left(c^\dagger_{1\mathbf{k}\uparrow} c_{2\mathbf{k}\uparrow} - c^\dagger_{1\mathbf{k}\downarrow} c_{2\mathbf{k}\downarrow} \right), \qquad \mathcal{O}_{CDW} = \sum_{\mathbf{k}} \left(c^\dagger_{1\mathbf{k}\uparrow} c_{2\mathbf{k}\uparrow} + c^\dagger_{1\mathbf{k}\downarrow} c_{2\mathbf{k}\downarrow} \right),$$

$$\mathcal{O}_{S} = \sum_{\mathbf{k}} \left(c^\dagger_{1\mathbf{k}\uparrow} c^\dagger_{1-\mathbf{k}\downarrow} + c^\dagger_{2\mathbf{k}\uparrow} c^\dagger_{2-\mathbf{k}\downarrow} \right), \qquad \mathcal{O}_{S^+} = \sum_{\mathbf{k}} \left(c^\dagger_{1\mathbf{k}\uparrow} c^\dagger_{1-\mathbf{k}\downarrow} - c^\dagger_{2\mathbf{k}\uparrow} c^\dagger_{2-\mathbf{k}\downarrow} \right).$$

- One-loop RG equations can be integrated analytically
- SDW and S^+ compete for the same portion of the FS ($CeIn_3$, $CePd_2Si_2$)

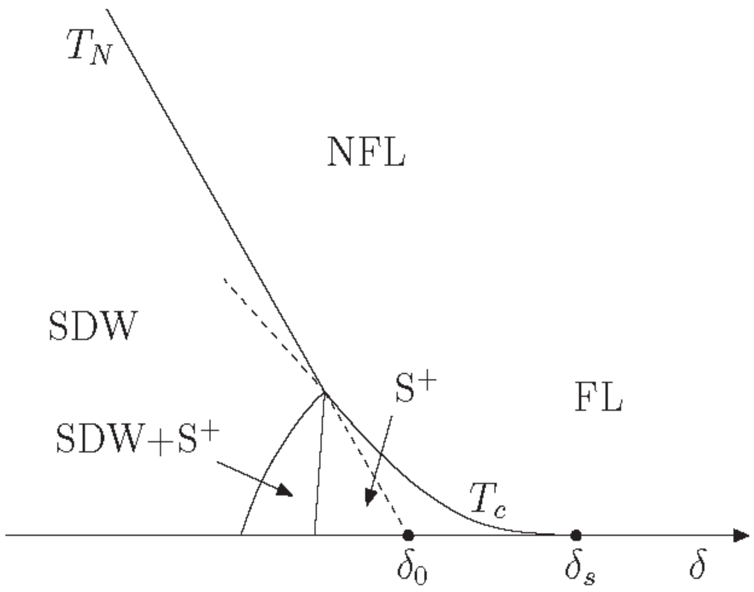

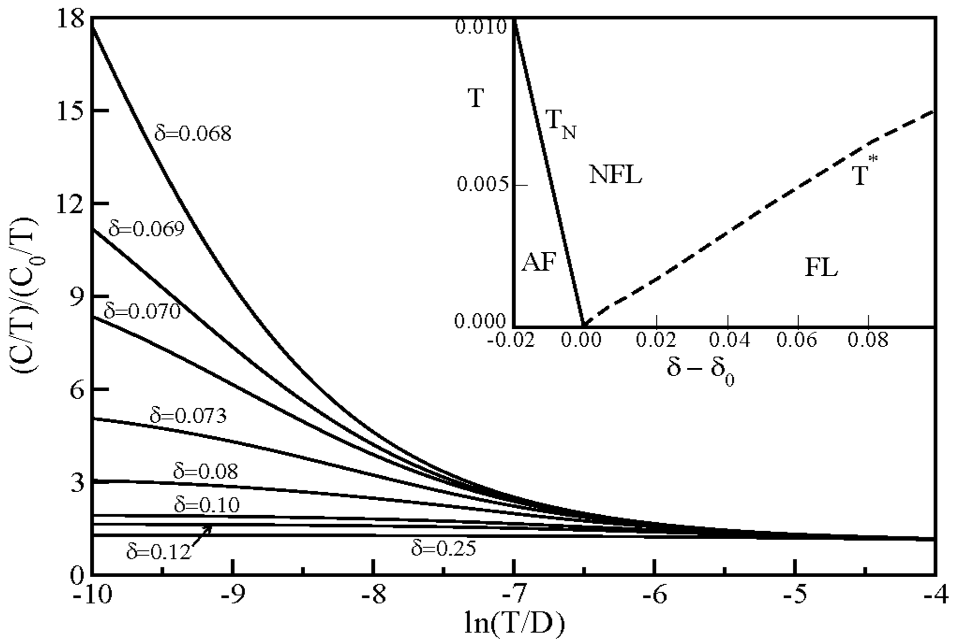

VI. Concluding remarks

- Perturbative RG limited to small and intermediate coupling.
  A strongly coupled system cannot return to weak coupling.
  Qualitatively correct even for strong coupling.
- T-dependence of C/T on logarithmic scale (as in experiment)
- Effective mass diverges at QCP (as for some systems)
- Resistivity linear or sublinear in T (as in experiment)
- Crossover from FL to NFL in C/T and ρ(T) (as in experiment)
- Deviations from Lorentzian Drude behavior
- Dynamical spin-susceptibility (neutron scattering) depends on geometry of Fermi surface and on **q**
- de Haas-van Alphen amplitudes strongly suppressed at the QCP (large effective mass)
- For Q=G/2 pairs of electrons can be transferred between pockets
  Superconducting dome above the QCP as in $CeIn_3$ and $CePd_2Si_2$
  Coexistence of SDW and S^+ superconductivity
- Two-band model is needed for localization (small vs large FS) and the dynamical susceptibility

Field-tuned QCP in $CeAuSb_2$

End-point of first order metamagnetic transition

analogous to $Sr_3Ru_2O_7$

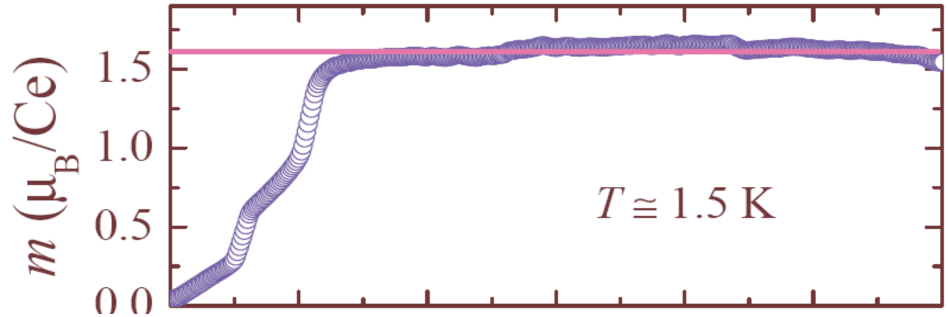

L. Balicas et al., Phys. Rev. B **72**, 064422 (2005)

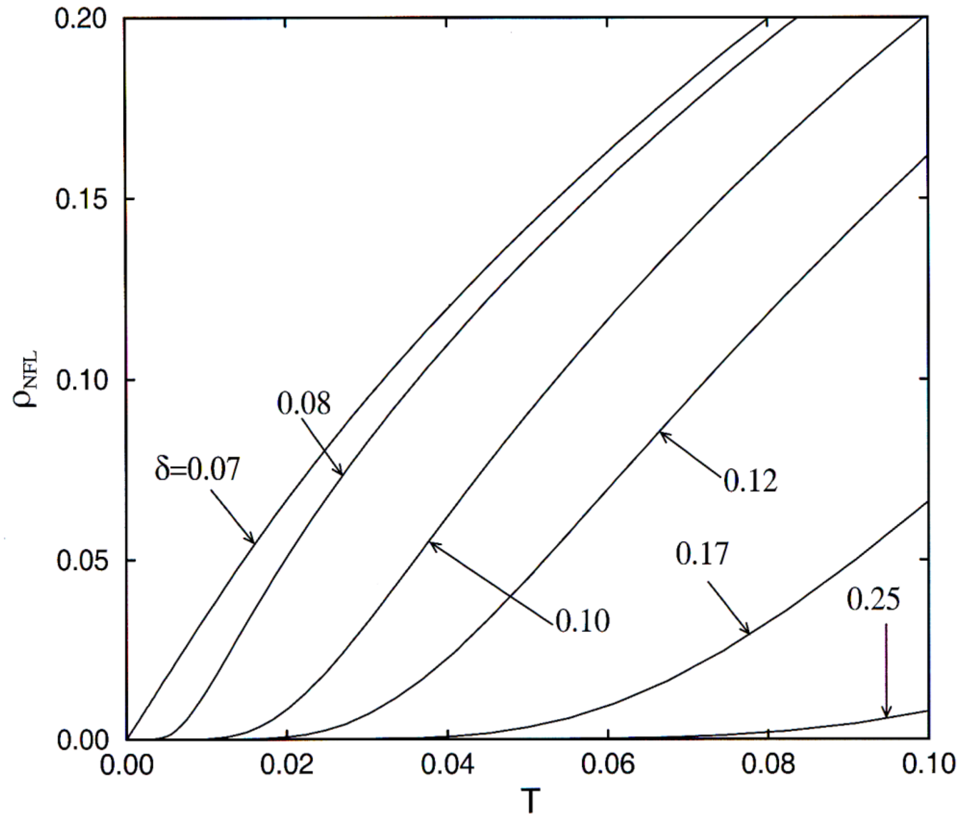

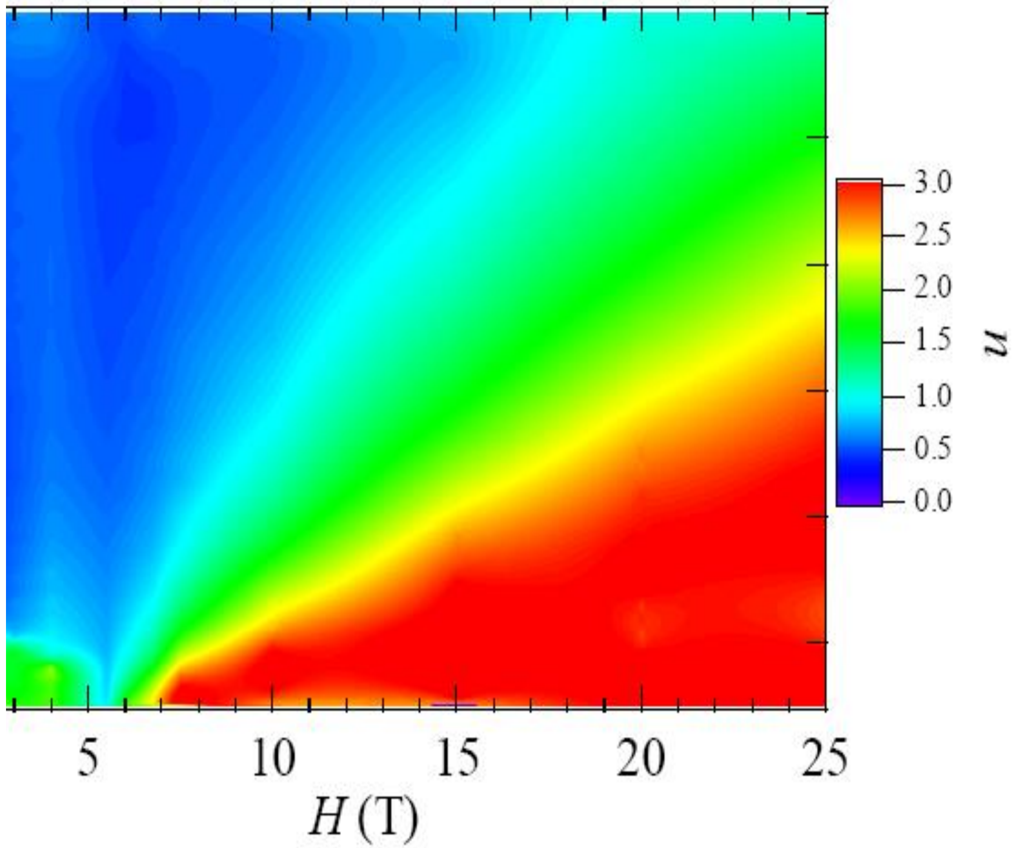

Resistivity

- NFL for tuned QCP
- Crossover from FL to NFL for $\delta > \delta_0$
- $\rho(T)$ roughly proportional to quasi-particle line width

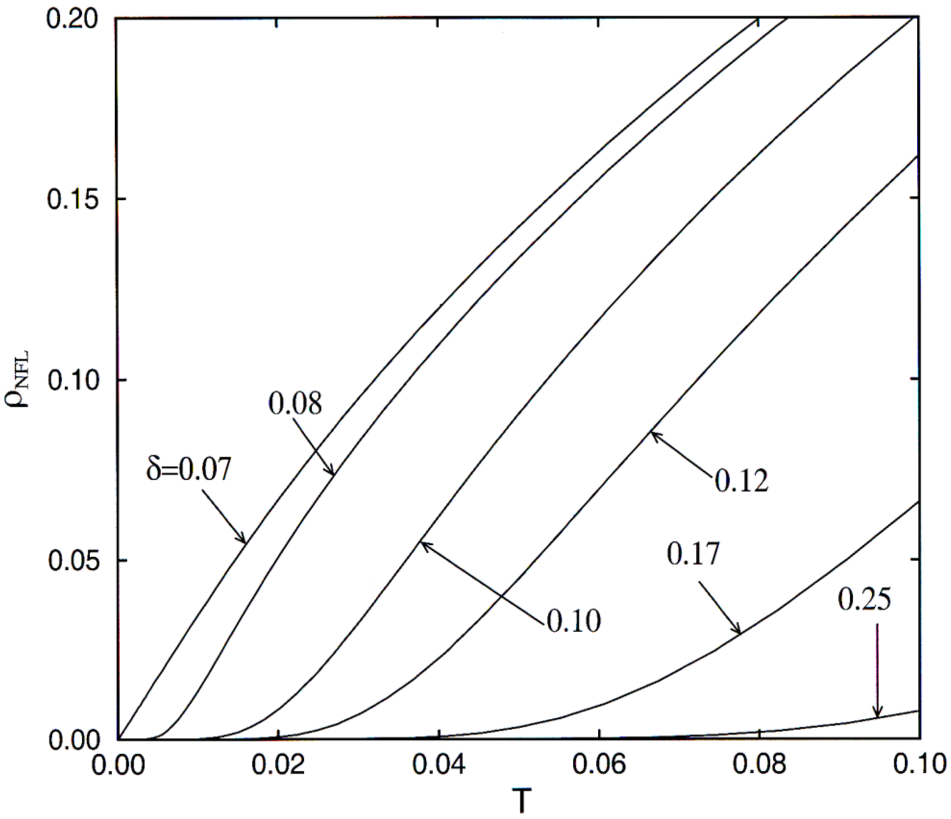

Dynamical conductivity

- Kubo formula
- Quasi-particles not well-defined for tuned QCP
- Plot $\omega\ \sigma(\omega)$
- Deviations from Drude behavior at low T

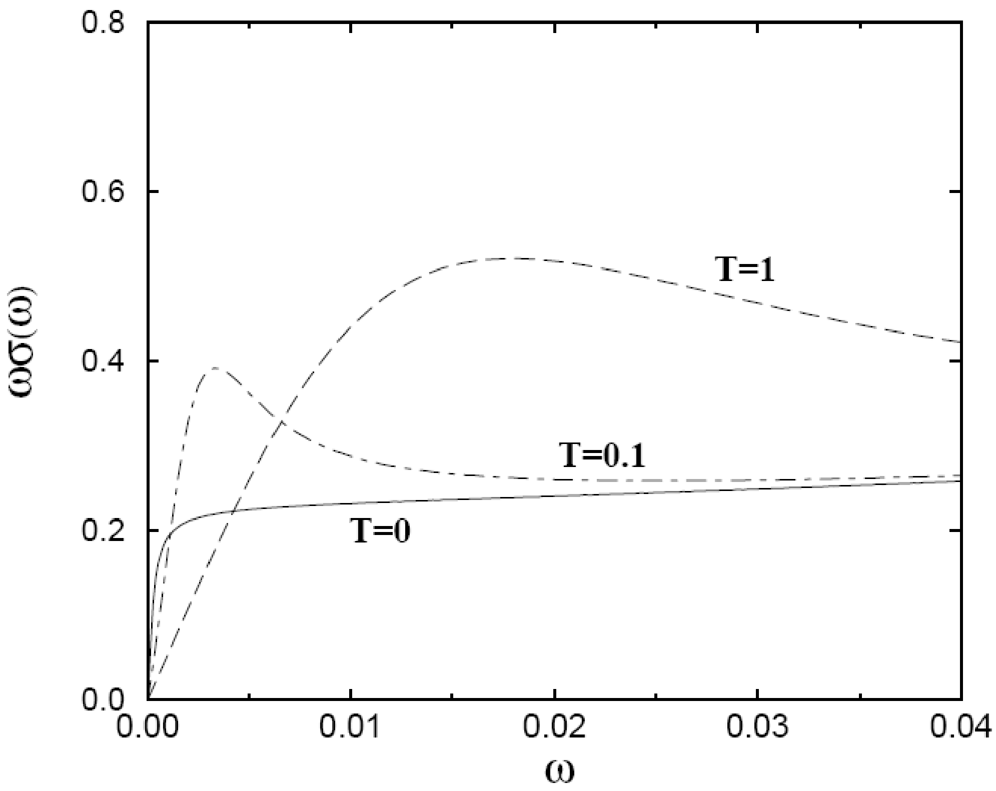

Staggered dynamical susceptibility

- Effective mass, quasi-particle lifetime and resistivity not very sensitive to geometry of FS, but X''(**Q**,ω)/ω is.
- Line-width proportional to T for tuned QCP
- No central peak for off-critical FS mismatch
- Differs from experiments
- Position and height of inelastic peak is function of δ and T

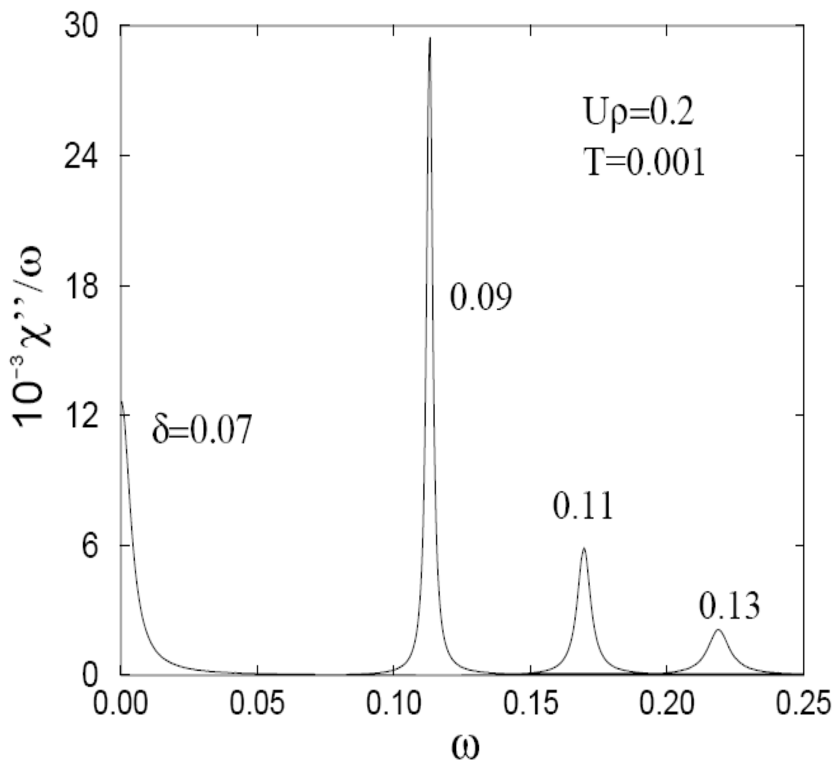

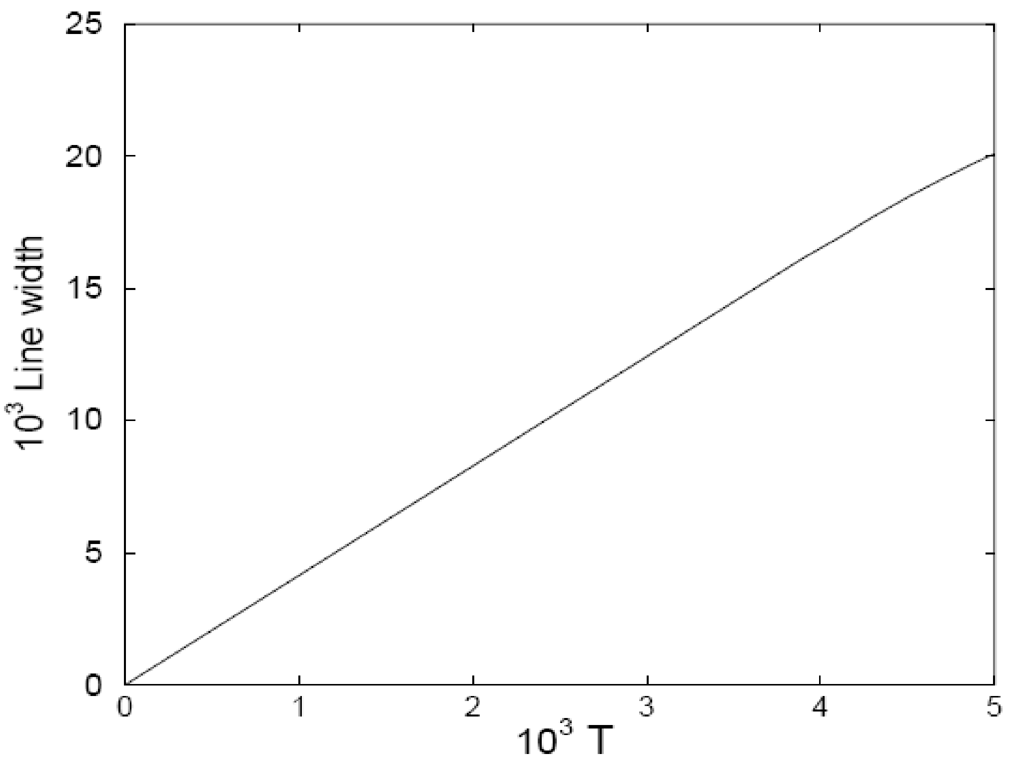

<u>Amplitudes of the dH-vA</u> oscillations for both pockets

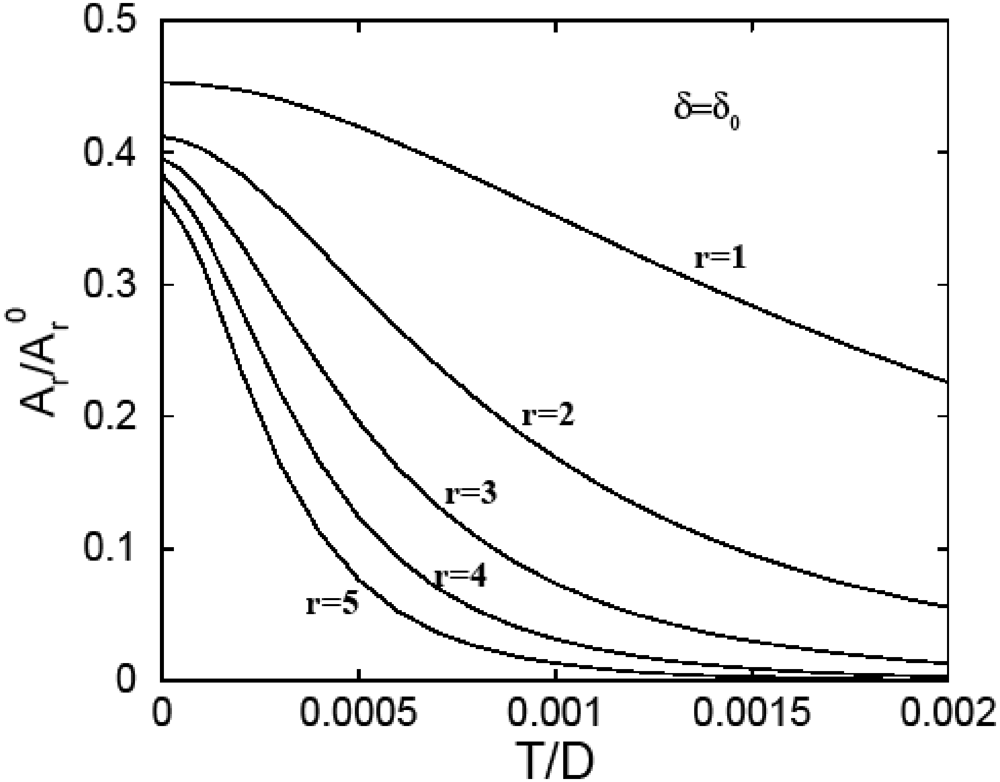

The amplitude is determined by the quasi-particle self-energy through a sum over Matsubara poles

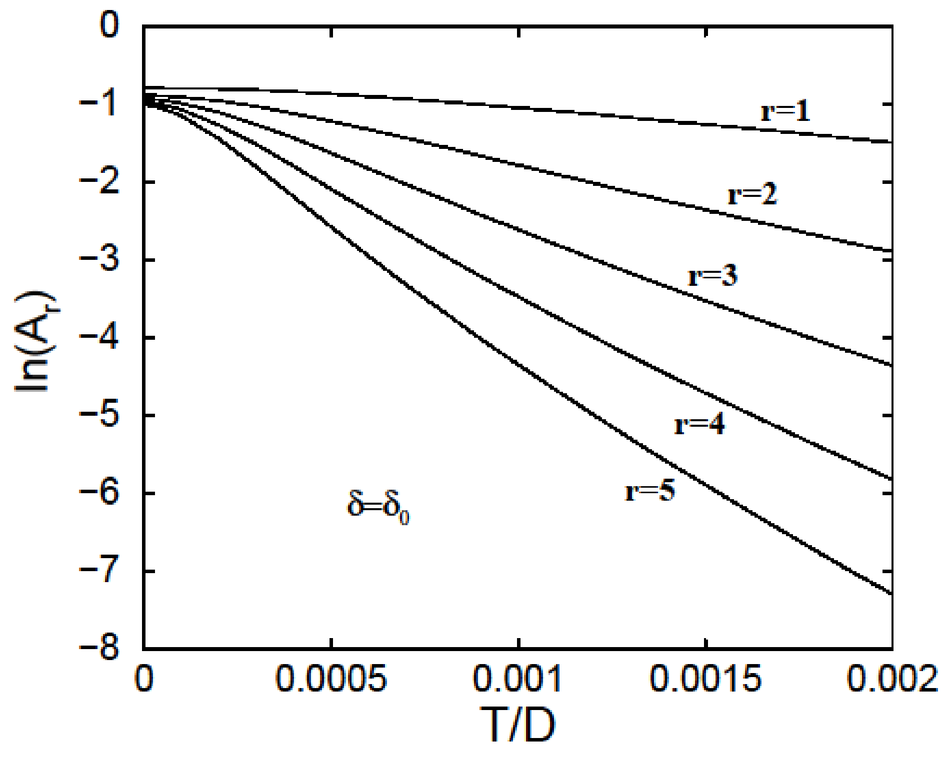

Amplitude strongly suppressed due to the heavy mass

r is index of the harmonic

B = 20 T m*/m = 10

Problem if B is tuning parameter

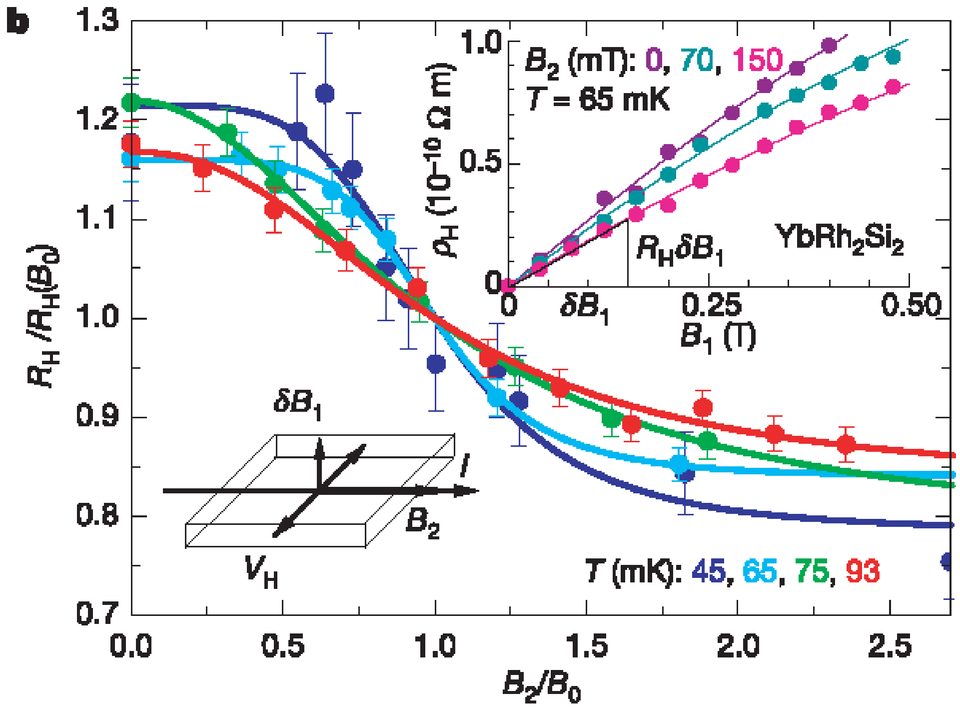

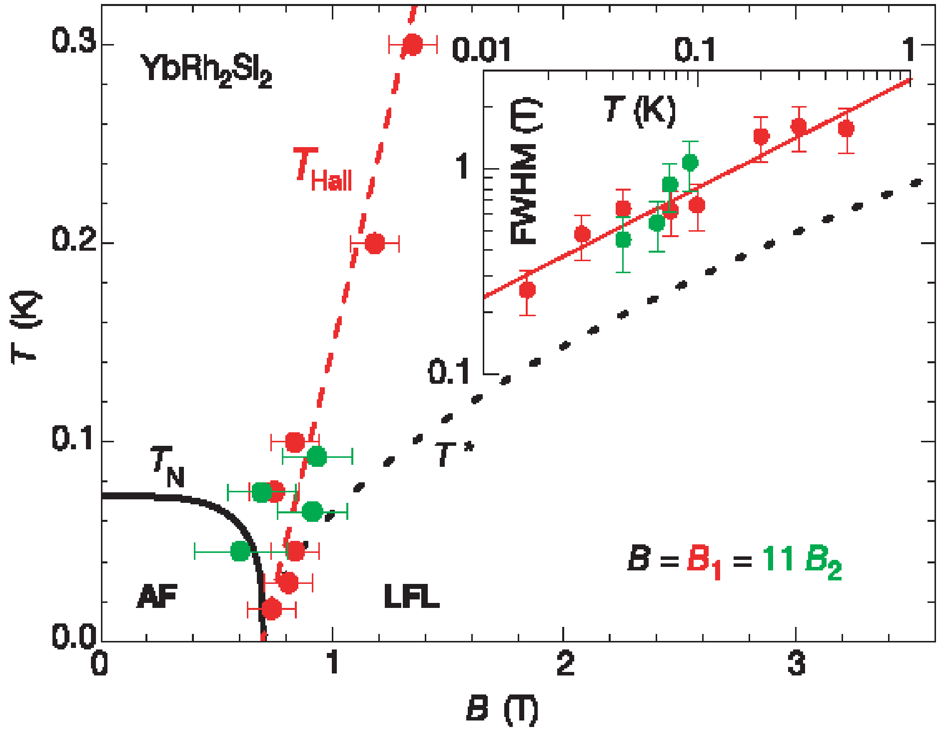

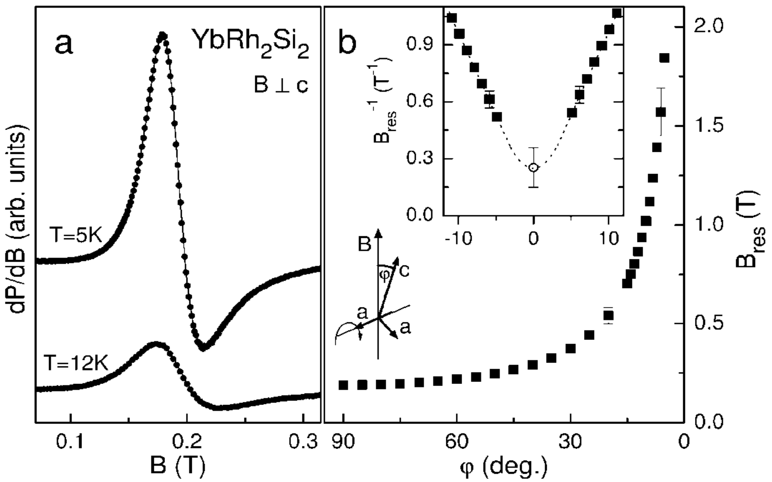

FIG. 1. (a) ESR spectra at 9.4 GHz (X band). Solid lines represent fits to the data with a Lorentzian line shape showing an asymmetry typical for metals. (b) Angle dependence of the resonance field B_{res} at $T = 5$ K. The single crystal is rotated in the magnetic field B as illustrated in the drawing. Inset: reciprocal B_{res} for $|\varphi| < 12°$. The dotted line is a guide to the eye that indicates the required vanishing of $dB_{res}/d\varphi$ at $\varphi = 0°$. The bar yields uncertainty for $B_{res}^{\|}(\varphi = 0°) \approx 4$ T.

YbRh$_2$Si$_2$: Hall effect and small vs large FS, Paschen et al Nature (2004)

ESR: Sichelschmidt et al PRL **91** (2003)

Why is there a resonance?

Abrahams + Wölfle, PRB **78** (2008)

Schlottmann, PRB **79** (2009)